Manipulability of Cooperating Robots with Unactuated Joints and Closed-Chain Mechanisms

Antonio Bicchi and Domenico Prattichizzo, *Member, IEEE*

***Abstract*—In this paper, we study the differential kinematics and the kineto-static manipulability indices of multiple cooperating robot arms, including active and passive joints. The kinematic manipulability indices are derived extending previous results on cooperating robots without passive joints. The force manipulability analysis for cooperative robot systems cannot be straightforwardly derived by "duality" arguments as it can with conventional arms, rather a distinction between active and passive force manipulability must be introduced. Results in this paper apply directly to the analysis of cooperating robots, parallel robots, dextrous robotic hands and legged vehicles, and, in general, to closed kinematic chains.**

***Index Terms*—Closed-chain mechanisms, cooperating robots, dextrous manipulation, kinematic and force manipulability, parallel robots.**

I. Introduction

SINCE their original proposition [13], [17], manipulability indices have been widely used in robotics analysis, task specification, and mechanism design. As is well known, the basic idea of manipulability analysis consists of describing directions in the task or joint space that extremize the ratio between some measure of effort in joint space and a measure of performance in task space. Whenever these measures are quadratic functions of the joint and task variables, respectively, and there is a linear relationship between the two sets of variables, then manipulability analysis amounts to the analysis of an eigenvalue-eigenvector problem. A typical result of such analysis is reported in Fig. 1, where the familiar ellipsoid representation in task space is used for velocity and force related performance/effort ratios. The extension of manipulability analysis to multiple cooperating robots has been studied by several authors so far. Lee [8] and Chiacchio *et al.* [5] proposed extensions for the case when all cooperating arms have full mobility in their task space. Bicchi *et al.* [1] extended the kinematic manipulability ellipsoid problem to general cooperating arms, with arbitrary number of joints per arm. Melchiorri [10] applied similar tools to address force manipulability in fully actuated mechanisms. The three papers [15], [11], [4] presented at the same conference session discussed different aspects of this problem. Wen and Wilfinger [15] (see also [16]) extended the concept of kinematic manipulability to general constrained rigid multibody systems including closed kinematic chains. Park and Kim [11] (see also [12]) studied manipulability of closed chains, including unactuated joints, using an elegant differential geometric formulation. The authors [4] (see also [3]) discussed the problem including effects of redundancy and indeterminacy of kinematics, and introduced the notion of active and passive force manipulability.

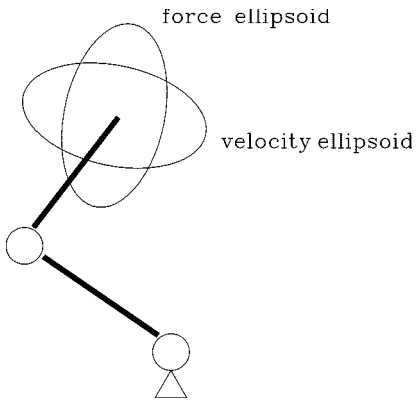

Fig. 1. Velocity and force ellipsoids in the task space of a serial-chain, fully actuated robot arm. By classical duality arguments, the principal directions are the same, while the lengths of axes are inversely proportional.

With respect to existing literature on the subject, the main contribution of this paper is threefold. Firstly, we explicitly describe a systematic procedure for building the kinematic model of a system of cooperating robots with passive joints, which can be used to attack a wide generality of mechanisms (such construction is only illustrated by particular examples in [15] and [11]). Secondly, by providing physical interpretations of manipulability results from different viewpoints (e.g., Yoshikawa's efficiency and Salisbury/Craig's accuracy viewpoints), we treat otherwise ill-posed kinematic redundancy and indeterminacy problems as optimization (or worst-case) problems. Finally, we propose a detailed study of manipulability in the force domain and show that a distinction between *active* and *passive* force manipulability must be introduced to obtain a full understanding of the characteristics of a closed-chain mechanism.

This paper is organized as follows. We preliminary show how several closed-chain problems can be solved by use of the formulation given in [1]. For cases when this is not possible, we introduce a generalization of those methods, which applies to general closed-chain systems (Section II). Manipulability indices are discussed in the kinematic domain in Section III, and in the force domain in Section IV. We conclude the paper by

Manuscript received January 19, 1999; revised November 9, 1999. This paper was recommended for publication by Associate Editor I. Walker and Editor S. Salcudean upon evaluation of the reviewers' comments. The work was supported in part by the ASI under Grant ARS-96-170 and MURST University of Pisa under Grant "Ramsete."

A. Bicchi is with the Centro Interdipartimentale di Ricerca "Enrico Piaggio," University of Pisa, 56100 Pisa, Italy (e-mail: bicchi@ing.unipi.it).

D. Prattichizzo is with the Dipartimento di Ingegneria dell'Informazione, University of Siena, 53100 Siena, Italy (e-mail: prattichizzo@ing.unisi.it).

Publisher Item Identifier S 1042-296X(00)06960-3.

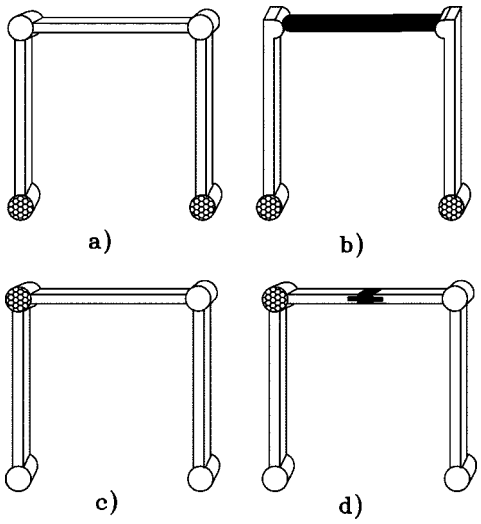

Fig. 2. The four-bar linkage (a) with unactuated joints (in white) adjacent to the reference member can be considered as a manipulation system and (b) with two one-joint fingers, one object (in black), and two soft-finger contacts. More generally, the four-bar linkage (c) can be represented as a manipulation system with two two-joint fingers, one object (in black), and two complete-constraint contacts.

illustrating applications of our results with two examples (Section V), where the proposed techniques are used to actually perform optimized design of closed-chain manipulators.

II. Problem Formulation

The approach we follow to analyze kinematics and statics of closed-chain mechanical system is to consider them as embodiments of a cooperative manipulation paradigm, where multiple robotic *limbs* (or fingers) interact with an *object* at a number of *contacts*. The object is the reference member of the mechanism, whose motions and forces are the ultimate goal of analysis. Contacts represent in fact unactuated kinematic pairs of different nature between the object and the contacting link, that restrict some or all the components of the relative velocities of the two bodies.

In [1], a notation for describing such systems was established which is recalled in Appendix A. In that paper, each limb is allowed an arbitrary number of joints. Contacts with the object are allowed at any link of the various limbs. Fig. 2(a) shows how a four-bar linkage with the two middle joints not actuated, and Fig. 2(b) shows how it can be thought of as a system of two cooperating fingers and an object, with two contacts of bilateral soft-finger type.[1] For more general cases, where the unactuated joints are not all adjacent to one element of the chain, e.g., Fig. 2(c), or when that element is not the member whose motions should be studied, methods of [1] have to be extended as described in the rest of this paper.

Consider a system of cooperating robotic limbs, comprised of q_a actuated joints, and q_p unactuated (passive) simple kinematic joints, which interact with an object at n contact points according to contact models as specified by a selection matrix $\mathbf{H}$ (see Appendix A). Let the aggregated Jacobian matrix of the cooperating devices be denoted $\tilde{\mathbf{J}}$, and let the object Jacobian (or grasp matrix) be $\tilde{\mathbf{G}}^T$. A suitable permutation matrix $\mathbf{P}$ can be found that reorders joint variables θ to have actuated joints on top, and unactuated joints at bottom, $\dot{\mathbf{q}}^T = [\dot{\mathbf{q}}_a^T \quad \dot{\mathbf{q}}_p^T] = \dot{\theta}^T \mathbf{P}^T$, where $\mathbf{q}_a$ (respectively, $\mathbf{q}_p$) is the q_a (q_p)-vector of actuated (unactuated) joint velocities. Correspondingly, the Jacobian matrix is partitioned as

$$\tilde{\mathbf{J}}\dot{\theta} = \tilde{\mathbf{J}}\mathbf{P}^{-1}\dot{\mathbf{q}} = \begin{bmatrix} \tilde{\mathbf{J}}_a & \tilde{\mathbf{J}}_p \end{bmatrix} \begin{bmatrix} \dot{\mathbf{q}}_a \\ \dot{\mathbf{q}}_p \end{bmatrix}.$$

The mobility of the system is then studied by analyzing the constraint equation

$$\begin{bmatrix} \mathbf{J}_a & \mathbf{J}_p & -\mathbf{G}^T \end{bmatrix} \begin{bmatrix} \dot{\mathbf{q}}_a \\ \dot{\mathbf{q}}_p \\ \dot{\mathbf{u}} \end{bmatrix} = \mathbf{0} \tag{1}$$

where $\mathbf{J}_a = \mathbf{H}\tilde{\mathbf{J}}_a$, $\mathbf{J}_p = \mathbf{H}\tilde{\mathbf{J}}_p$ and $\mathbf{G}^T = \mathbf{H}\tilde{\mathbf{G}}^T$. All possible motions of the system belong to the nullspace (or kernel) of the constraint matrix $[\mathbf{J}_a \quad \mathbf{J}_p \quad -\mathbf{G}^T]$ and, hence, can be rewritten as linear combinations of vectors forming a basis of the nullspace. By suitable linear algebra operations (see, e.g., [1]), such a basis can always be written in a block-partitioned form

$$\left[\begin{array}{c} \dot{\mathbf{q}}_a \\ \hline \dot{\mathbf{q}}_p \\ \dot{\mathbf{u}} \end{array}\right] = \left[\begin{array}{c|cc} \boldsymbol{\Gamma}_{a,r} & \boldsymbol{\Gamma}_{a,c} & \mathbf{0} \\ \hline \mathbf{0} & \boldsymbol{\Gamma}_{po,c} & \boldsymbol{\Gamma}_i \end{array}\right] \left[\begin{array}{c} \mathbf{x}_1 \\ \hline \mathbf{x}_2 \\ \mathbf{x}_3 \end{array}\right]. \tag{2}$$

In (2), $\boldsymbol{\Gamma}_{a,r}$ is a basis matrix of $\ker(\mathbf{J}_a)$ and incorporates the redundancy[2] of the actuated part of the mechanism: all possible rigid-body motions of the actuated joints when both the reference member and the passive joints are locked can be written as linear combinations of columns of $\boldsymbol{\Gamma}_{a,r}$. Conversely, $\boldsymbol{\Gamma}_i = \ker[\mathbf{J}_p, -\mathbf{G}^T]$ in (2) represents all possible motions of the system, when actuated joints are locked. We will refer to the column space of $\boldsymbol{\Gamma}_i$ as the *kinematic indeterminacy* subspace of the mechanisms at the given configuration.[3] The second block column of the matrix in (2) characterizes the coordinate motions of the system. Vectors $\boldsymbol{\Gamma}_{po,c}\mathbf{x}_2$ represent the unique possible motion of the passive joints and of the object, coordinated with motions $\boldsymbol{\Gamma}_{a,c}\mathbf{x}_2$ of actuated joint.

A finer partition of block matrices in (2) provides a more detailed analysis of mobility of systems under investigation. By some algebraic manipulation, the indeterminate motion term can be rewritten as

$$\boldsymbol{\Gamma}_i \mathbf{x}_3 = \begin{bmatrix} \boldsymbol{\Gamma}_{p,r} & \boldsymbol{\Gamma}_{po,i} & \mathbf{0} \\ \mathbf{0} & \boldsymbol{\Gamma}_{op,i} & \boldsymbol{\Gamma}_{o,i} \end{bmatrix} \begin{bmatrix} \mathbf{x}_{31} \\ \mathbf{x}_{32} \\ \mathbf{x}_{33} \end{bmatrix}. \tag{3}$$

Here, $\boldsymbol{\Gamma}_{p,r} = \ker(\mathbf{J}_p)$ incorporates all motions of passive joints which are free (redundant) when both active joints and reference member (object) locked (as, e.g., in a Stewart platform whose legs can rotate freely about the spherical joints at their extremities). On the other hand, $\boldsymbol{\Gamma}_{o,i} = \ker(\mathbf{G}^T)$ represents motions

[1] Soft-finger contacts prevent all relative linear velocities, and allow relative angular velocities in the plane of contact, see Appendix A.

[2] As a variable naming convention, we use subscripts with the initial letter of the relevant keyword. The letter is underlined at the first occurrence of the keyword.

[3] The term *instability* is used in [16]. We prefer to avoid reference to stability concepts in this quasi-static setting. Furthermore, the dual case in the force domain is customarily defined as *static indeterminacy*.

of the object that are indeterminate, i.e., not constrained (up to first order), when all joints, active and passive, are locked. The passive joint motions that lie in the image (or column space) of $\mathbf{\Gamma}_{po,\,i}$ correspond one-to-one to object motions in the image of $\mathbf{\Gamma}_{op,\,i}$ when active joints are locked (hence are kinematically indeterminate). Kinematic indeterminacy with nonvoid blocks $\mathbf{\Gamma}_{po,\,i}$, $\mathbf{\Gamma}_{op,\,i}$ and $\mathbf{\Gamma}_{o,\,i}$ imply that the velocity of the task frame fixed to the object is not uniquely determined when active joints velocities are, hence typically represent an undesirable condition which may be obtained at singular configurations.

The second block column in (2) can also be rewritten as

$$\left[\begin{array}{c}\mathbf{\Gamma}_{a,\,c}\\ \hline \mathbf{\Gamma}_{op,\,c}\end{array}\right]\mathbf{x}_2=\left[\begin{array}{ccc}\mathbf{\Gamma}_{ap,\,c} & \mathbf{\Gamma}_{apo,\,c} & \mathbf{\Gamma}_{ao,\,c}\\ \hline \mathbf{\Gamma}_{pa,\,c} & \mathbf{\Gamma}_{poa,\,c} & \mathbf{0}\\ \mathbf{0} & \mathbf{\Gamma}_{opa,\,c} & \mathbf{\Gamma}_{oa,\,c}\end{array}\right]\left[\begin{array}{c}\mathbf{x}_{21}\\ \mathbf{x}_{22}\\ \mathbf{x}_{23}\end{array}\right] \tag{4}$$

showing: coordinate motions of the actuated and passive joints while the object is locked (first block column); coordinate motions of actuated joints and object with locked unactuated joints (third block column); and motions that are only possible by coordinated simultaneous movement of object, active and passive joints (second block column).

Summarizing results of (2)–(4), a kinematic description of all possible motions of a general closed-chain mechanism can be given in (5), shown at the bottom of the page, where $\mathbf{x}=[\mathbf{x}_1^T\mathbf{x}_{21}^T\mathbf{x}_{22}^T\mathbf{x}_{23}^T\mathbf{x}_{31}^T\mathbf{x}_{32}^T\mathbf{x}_{33}^T]^T$.

The method of analysis based on the cooperative robots paradigm as described in this section can be applied to general closed kinematic chains. For example, to the four-bar linkage of Fig. 2(c), where the only actuated joint is in the middle of the chain. An equivalent manipulation system is depicted in Fig. 2(d), for the case when the reference member of interest in the linkage is its middle link. The system is now regarded as being comprised of two limbs with two joints, three of which are unactuated (in white), and an object (in black) grasped by two completely constraining contacts. Other examples of application to a five-bar linkage and to a Stewart platform are reported in Section V.

III. Kinematic Manipulability

A kinematic manipulability index, in the sense of Yoshikawa [17], can be defined in terms of the ratio of a measure of performance in the task space and a measure of effort in the joint space. Taking these measures to be suitably defined two-norms of velocities, an index can be written as

$$R_k=\frac{\dot{\mathbf{u}}^T\mathbf{W}_u\dot{\mathbf{u}}}{\dot{\mathbf{q}}^T\mathbf{W}_q\dot{\mathbf{q}}} \tag{6}$$

where $\mathbf{W}_u$, $\mathbf{W}_q$ are positive definite matrices whose role is to weight different components of velocities in the two spaces (including the case of nonhomogeneous units for linear or angular velocities). Observe that this choice of weights effectively amounts to defining a metric on the tangent space to the task and joint manifolds [12]. In practice, the choice of $\mathbf{W}_q$ is made based on how much it "costs" to run a certain actuator at unit velocity. The choice of $\mathbf{W}_u$ is usually made based on the task specifications (see, e.g., [18] and Section V).

It should also be pointed out that a different interpretation of manipulability indices is possible, in the original spirit of the work of Salisbury and Craig [13], as one can consider differential motions instead of velocities, and regard

$$R_k=\frac{\delta\mathbf{u}^T\mathbf{W}_u\delta\mathbf{u}}{\delta\mathbf{q}^T\mathbf{W}_q\delta\mathbf{q}} \tag{7}$$

as the ratio between a norm of errors in positioning the end-effector $\delta\mathbf{u}$, and a norm of errors $\delta\mathbf{q}$ in controlling the joints to their set-points (the latter errors being regarded as causes of the former, and both being considered small enough to be approximated with their differential). The analytic formulation of the Yoshikawa's problem and the Salisbury–Craig problem are quite similar, although different interpretations of results are in order (typically, what is a "good" direction for one problem is "bad" for the other).

As we are interested in performance in the space of velocities of the reference member $\dot{\mathbf{u}}$, and efforts (or errors) in the space of actuated (and measured) joints, the index (6) is rewritten as

$$R_{ak}=\frac{\dot{\mathbf{u}}^T\mathbf{W}_u\dot{\mathbf{u}}}{\dot{\mathbf{q}}_a^T\mathbf{W}_q\dot{\mathbf{q}}_a}. \tag{8}$$

The analysis of which directions in the task space (and corresponding directions in the actuated joint space) maximize or minimize R_{ak} is easily solved once a correspondence between the numerator and denominator variables, namely $\dot{\mathbf{u}}$ and $\dot{\mathbf{q}}_a$, in (8) is established. Note that in order for ratio (6) to be well-defined, a one-to-one mapping should be established between the two variables. To find such mapping, rewrite (5) as

$$\left\{\begin{array}{ll}\dot{\mathbf{q}}_a &= \mathbf{\Gamma}_{a,\,r}\mathbf{x}_1+\mathbf{\Gamma}_{ap,\,c}\mathbf{x}_{21}+\mathbf{\Gamma}_{apo,\,c}\mathbf{x}_{22}+\mathbf{\Gamma}_{ao,\,c}\mathbf{x}_{23}\\ &= \mathbf{\Gamma}_r\mathbf{x}_r+\mathbf{\Gamma}_{q,\,c}\mathbf{x}_c\\ \dot{\mathbf{u}} &= \mathbf{\Gamma}_{opa,\,c}\mathbf{x}_{22}+\mathbf{\Gamma}_{oa,\,c}\mathbf{x}_{23}+\mathbf{\Gamma}_{op,\,i}\mathbf{x}_{32}+\mathbf{\Gamma}_{o,\,i}\mathbf{x}_{33}\\ &= \mathbf{\Gamma}_{o,\,c}\mathbf{x}_c+\mathbf{\Gamma}_{ii}\mathbf{x}_i\end{array}\right. \tag{9}$$

where

$$\begin{aligned}\mathbf{\Gamma}_r &\stackrel{\text{def}}{=}[\mathbf{\Gamma}_{a,\,r}\mathbf{\Gamma}_{ap,\,c}] \qquad \mathbf{\Gamma}_{q,\,c}\stackrel{\text{def}}{=}[\mathbf{\Gamma}_{apo,\,c}\mathbf{\Gamma}_{ao,\,c}]\\ \mathbf{\Gamma}_{o,\,c} &\stackrel{\text{def}}{=}[\mathbf{\Gamma}_{opa,\,c}\mathbf{\Gamma}_{oa,\,c}] \qquad \mathbf{\Gamma}_{ii}\stackrel{\text{def}}{=}[\mathbf{\Gamma}_{op,\,i}\mathbf{\Gamma}_{o,\,i}]\end{aligned} \tag{10}$$

and vectors $\mathbf{x}_r$, $\mathbf{x}_i$, and $\mathbf{x}_c$ parameterize unconstrained motions of active joints when the reference member is locked, object motions when active joints are locked, and coordinate motions of active joints and object, respectively.

$$\left[\begin{array}{c}\dot{\mathbf{q}}_a\\ \hline \dot{\mathbf{q}}_p\\ \dot{\mathbf{u}}\end{array}\right]=\left[\begin{array}{c|ccc|ccc}\mathbf{\Gamma}_{a,\,r} & \mathbf{\Gamma}_{ap,\,c} & \mathbf{\Gamma}_{apo,\,c} & \mathbf{\Gamma}_{ao,\,c} & \mathbf{0} & \mathbf{0} & \mathbf{0}\\ \hline \mathbf{0} & \mathbf{\Gamma}_{pa,\,c} & \mathbf{\Gamma}_{poa,\,c} & \mathbf{0} & \mathbf{\Gamma}_{p,\,r} & \mathbf{\Gamma}_{po,\,i} & \mathbf{0}\\ \mathbf{0} & \mathbf{0} & \mathbf{\Gamma}_{opa,\,c} & \mathbf{\Gamma}_{oa,\,c} & \mathbf{0} & \mathbf{\Gamma}_{op,\,i} & \mathbf{\Gamma}_{o,\,i}\end{array}\right]\mathbf{x} \tag{5}$$

From (9), it appears that a one-to-one relationship between task and actuated joints velocities does not exist in general, because of the possible presence of redundancy (matrix $\mathbf{\Gamma}_r$) and indeterminacy (matrix $\mathbf{\Gamma}_{ii}$). This problem can be circumvented if the physical interpretation of manipulability ratios is taken into account.

Consider first the case that there is redundancy, but no indeterminacy ($\mathbf{\Gamma}_{ii} = \mathbf{0}$). From Yoshikawa's viewpoint, it is reasonable to assume that if more than one actuated joint velocity can be chosen corresponding to some task velocity, then the one with minimum cost will be preferred in the controller policy (different redundancy resolution schemes can be accommodated for by suitable choices of the cost weights $\mathbf{W}_q$). We might then redefine an *optimized* efficiency ratio (8) for redundant systems as

$$R_{ak}^{o\text{-}red} = \frac{\dot{\mathbf{u}}^T \mathbf{W}_u \dot{\mathbf{u}}}{\min_{\mathbf{x}_r} \dot{\mathbf{q}}_a^T \mathbf{W}_q \dot{\mathbf{q}}_a}. \tag{11}$$

From the Salisbury–Craig's viewpoint, redundancy of actuation should conservatively be taken into account as if playing against the mechanism accuracy, hence by considering the *worst-case* controller error $\delta\mathbf{q}$ which, among those compatible with a given $\delta\mathbf{u}$, minimizes the denominator. Thus, the same mathematical problem of (11) is obtained, with a very different physical interpretation. The constrained minimization problem appearing in the denominator of (11) can be readily solved by standard linear algebraic tools (see, e.g., [14]). Since we will often meet in the sequel similar problems, we introduce a specific notation for the *projector matrix* $\mathbf{P}_{(\mathbf{A},\,Q)} \stackrel{\text{def}}{=} \mathbf{I} - \mathbf{A}\mathbf{A}_Q^+$ [where $\mathbf{A}_Q^+ \stackrel{\text{def}}{=} (\mathbf{A}^T\mathbf{Q}\mathbf{A})^{-1}\mathbf{A}^T\mathbf{Q}$ denotes the $\mathbf{Q}$-weighted pseudoinverse of $\mathbf{A}$], such that the quadratic form $\mathbf{x}^T\mathbf{Q}\mathbf{x}$ subject to the linear constraint $\mathbf{x} = \mathbf{A}\mathbf{y} + \mathbf{b}$ has its global minimum in $\hat{\mathbf{x}} = \mathbf{P}_{(\mathbf{A},\,Q)}\mathbf{b}$. We have therefore that the minimum of the denominator of (11) is

$$\min_{\mathbf{x}_r} \dot{\mathbf{q}}^T \mathbf{W}_q \dot{\mathbf{q}} = \mathbf{x}_c^T \mathbf{\Gamma}_{qc}^T \mathbf{P}_{(\mathbf{\Gamma}_r,\,W_q)}^T \mathbf{W}_q \mathbf{P}_{(\mathbf{\Gamma}_r,\,W_q)} \mathbf{\Gamma}_{qc} \mathbf{x}_c.$$

Hence, the kinematic manipulability analysis in the presence of passive joints and redundancy is reduced to studying the ratio

$$R_{ak}^{o\text{-}red} = \frac{\mathbf{x}_c^T \mathbf{\Gamma}_{oc}^T \mathbf{W}_u \mathbf{\Gamma}_{oc} \mathbf{x}_c}{\mathbf{x}_c^T \mathbf{\Gamma}_{qc}^T \mathbf{P}_{(\mathbf{\Gamma}_r,\,W_q)}^T \mathbf{W}_q \mathbf{P}_{(\mathbf{\Gamma}_r,\,W_q)} \mathbf{\Gamma}_{qc} \mathbf{x}_c} \tag{12}$$

at varying $\mathbf{x}_c$, i.e., a generalized eigenvalue problem [6].

The case that the system is kinematically indeterminate ($\mathbf{\Gamma}_{ii} \neq \mathbf{0}$) is of practical interest at the singularities of the mechanism. Because of the existence of nonzero task frame twists corresponding to zero active joint velocities, the efficiency index in (11) results unbounded. From the Salisbury–Craig viewpoint, this means that near-singular configurations are very inaccurate. In Yoshikawa's perspective, however, where (11) represents a performance, only a worst-case approach would make sense, whereby the least feasible object velocity is assumed to occur for a given active joint velocity. A manipulability ratio for kinematically redundant and indeterminate mechanisms, which is *optimized* w.r.t. redundancy and *worst-case* w.r.t. indeterminacy, is thus defined as

$$\begin{aligned} R_k^{ow} &= \frac{\min_{\mathbf{x}_i} \dot{\mathbf{u}}^T \mathbf{W}_u \dot{\mathbf{u}}}{\min_{\mathbf{x}_r} \dot{\mathbf{q}}_a^T \mathbf{W}_q \dot{\mathbf{q}}_a} \\ &= \frac{\mathbf{x}_c^T \mathbf{\Gamma}_{oc}^T \mathbf{P}_{(\mathbf{\Gamma}_{ii},\,W_u)}^T \mathbf{W}_u \mathbf{P}_{(\mathbf{\Gamma}_{ii},\,W_u)} \mathbf{\Gamma}_{oc} \mathbf{x}_c}{\mathbf{x}_c^T \mathbf{\Gamma}_{qc}^T \mathbf{P}_{(\mathbf{\Gamma}_r,\,W_q)}^T \mathbf{W}_q \mathbf{P}_{(\mathbf{\Gamma}_r,\,W_q)} \mathbf{\Gamma}_{qc} \mathbf{x}_c}. \end{aligned} \tag{13}$$

IV. Force Manipulability

The force manipulability index is similarly defined as the ratio of a performance measure in the space of forces exchanged with the environment, and an effort measure in the space of actuated joint torques

$$R_{af} = \frac{\mathbf{w}^T \mathbf{W}_w \mathbf{w}}{\boldsymbol{\tau}_a^T \mathbf{W}_\tau \boldsymbol{\tau}_a}. \tag{14}$$

Here, weights in $\mathbf{W}_\tau$ incorporate different costs in generating torque or forces at joints, and takes care of mismatches of measurement units between rotational and prismatic joints. Weights in $\mathbf{W}_w$ adjust for different units of components of the six-dimensional wrench $\mathbf{w}$, and may represent task specifications (such as greater leverage in some direction). A physically motivated choice could be taking $\mathbf{W}_w$ as the stiffness matrix of the environment with which the reference member interacts.[4]

From application of the virtual work principle, the relation between wrenches on the reference member $\mathbf{w}$ and the vector $\mathbf{f}$ of contact forces at equilibrium is $\mathbf{w} = \mathbf{G}\mathbf{f}$, while actuated joint torques $\boldsymbol{\tau}_a$ are related to contact forces as $\boldsymbol{\tau}_a = -\mathbf{J}_a^T\mathbf{f}$. Furthermore, the fact that no torque is applied at passive joints is expressed as $\mathbf{J}_p^T\mathbf{f} = \mathbf{0}$. These relations can be rewritten in matrix form as

$$\begin{bmatrix} \mathbf{I} & \mathbf{0} & -\mathbf{G} \\ \mathbf{0} & \mathbf{I} & \mathbf{J}_a^T \\ \mathbf{0} & \mathbf{0} & \mathbf{J}_p^T \end{bmatrix} \begin{bmatrix} \mathbf{w} \\ \boldsymbol{\tau}_a \\ \mathbf{f} \end{bmatrix} = \mathbf{0}. \tag{15}$$

Remark: For a static equilibrium to be possible with unrestricted active joint torques, it is necessary and sufficient that wrenches applied on the reference member satisfy

$$\mathbf{w} \in \mathtt{range}\left(\mathbf{G}\ \ker\left(\mathbf{J}_p^T\right)\right). \tag{16}$$

The possibility for the mechanism to balance an arbitrary wrench $\mathbf{w}$ is naturally related to the kinematic indeterminacy of the system. In fact, condition (16) for all $\mathbf{w}$ implies

$$\ker\left(\mathbf{G}^T\right) = \mathbf{0} \tag{17}$$

$$\mathtt{range}\left(\mathbf{G}^T\right) \cap \mathtt{range}\left(\mathbf{J}_p\right) = \mathbf{0} \tag{18}$$

and this in turn implies that blocks $\mathbf{\Gamma}_{po,\,i}$, $\mathbf{\Gamma}_{op,\,i}$, and $\mathbf{\Gamma}_{o,\,i}$ are void in (3). Redundancy in passive joints [corresponding to a nonvoid block $\mathbf{\Gamma}_{p,\,r}$ in (3)] does not influence the possibility of balancing arbitrary external wrenches.

In the grasping literature, contact forces in the nullspace of $\mathbf{G}$ are usually referred to as *internal* (or *homogeneous*) forces, which physically represent forces that do not affect the balance

[4] In this case, the numerator of (14) would represent twice the elastic energy of interaction.

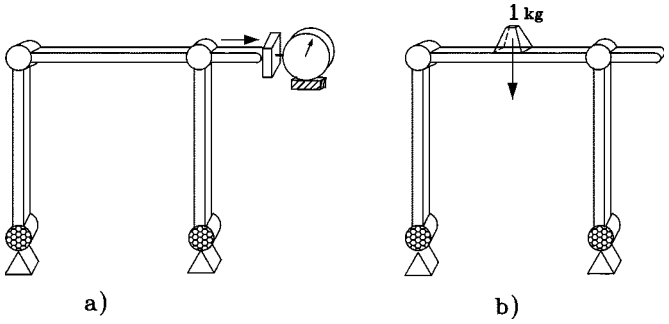

Fig. 3. A cooperating system may actively exert a wrench (a) and passively resist an external wrench (b) with best efficiency in different directions.

of the object; we will also refer to contact forces that lie both in the nullspace of $\mathbf{J}_a^T$ and in the nullspace of $\mathbf{J}_p^T$ (i.e., forces at the contact points that do not affect the balance of the limbs) as to *structural* forces. A mechanism is called *statically indeterminate* if $\ker(\mathbf{G}) \cap \ker(\mathbf{J}_a^T) \neq \mathbf{0}$. If (and only if) the system is not statically indeterminate, all equilibrium combinations of external wrenches and active joint torques solving (15) can be obtained by an algorithm similar to that used in Section II and described in [1], in the form

$$\begin{bmatrix} \mathbf{w} \\ \boldsymbol{\tau}_a \\ \mathbf{f} \end{bmatrix} = \begin{bmatrix} \mathbf{0} & \boldsymbol{\Gamma}_w & \boldsymbol{\Gamma}_s \\ \boldsymbol{\Gamma}_h & \boldsymbol{\Gamma}_\tau & \mathbf{0} \\ \boldsymbol{\Gamma}_{fh} & \boldsymbol{\Gamma}_f & \boldsymbol{\Gamma}_{fs} \end{bmatrix} \begin{bmatrix} \mathbf{x}_h \\ \mathbf{x}_a \\ \mathbf{x}_s \end{bmatrix}. \tag{19}$$

Notice that a similar decomposition of forces was used by [10], although passive joints and statically indeterminate systems were not considered. Here, contact forces such as $\boldsymbol{\Gamma}_{fh}\mathbf{x}_h$ [which belong to $\ker(\mathbf{G}) \cap \ker(\mathbf{J}_p^T)$] represent active internal (or h*omogeneous*) forces that do not affect the balance of the object, nor the passive joints; such internal forces are counterbalanced by torques at the active joints $\boldsymbol{\Gamma}_h\mathbf{x}_h$. On the other hand, contact forces such as $\boldsymbol{\Gamma}_{fs}\mathbf{x}_s$ [belonging to $\ker(\mathbf{J}_a^T) \cap \ker(\mathbf{J}_p^T)$] represent structural contact forces that are balanced by zero torques at the joints and by wrenches on the object $\boldsymbol{\Gamma}_s\mathbf{x}_s$. Finally, the second block column of the matrix in (19) characterizes the actual force transmission from active joint torques to object wrenches, and vice versa: wrenches such as $\boldsymbol{\Gamma}_w\mathbf{x}_a$ represent the unique possible wrench on the object corresponding to actuated joint torques $\boldsymbol{\Gamma}_\tau\mathbf{x}_a$, and both uniquely correspond to contact forces $\boldsymbol{\Gamma}_f\mathbf{x}_a$. Notice that the decomposition in (19) can always be made such that blocks in the same row are mutually orthogonal w.r.t. the internal product defined on their range space, such that $\boldsymbol{\Gamma}_w^T\mathbf{W}_w\boldsymbol{\Gamma}_s = 0$, $\boldsymbol{\Gamma}_h^T\mathbf{W}_\tau\boldsymbol{\Gamma}_\tau = 0$.

In dealing with force manipulability analysis for closed kinematic chains, it is necessary to introduce a finer discussion of different types of performance indices and costs associated with different tasks. In particular, a distinction between *active* and *passive* force manipulability should be introduced. The motivation for such a distinction clearly results by observing the simple examples described in Fig. 3. It appears that the wrenches that a manipulation system is able to apply most efficiently through the object to the environment, may differ from wrenches that are most efficiently resisted if external loads act on the object. It is then natural to introduce two distinct force manipulability indices.

A. Active Force Manipulability

For a given set of equilibrium torques at the actuated joints, i.e., for given $\mathbf{x}_a$ and $\mathbf{x}_h$ in (19), the corresponding wrench is not uniquely defined if a nullspace of $\mathbf{J}^T = [\mathbf{J}_a \quad \mathbf{J}_p]^T$ exists. However, in the worst case (when wrenches $\mathbf{w}$ are considered to play against maximization of the index), efficiency will be given by

$$R_{af}^w = \frac{\min_{\mathbf{x}_s} \mathbf{w}^T\mathbf{W}_w\mathbf{w}}{\boldsymbol{\tau}_a^T\mathbf{W}_\tau\boldsymbol{\tau}_a}. \tag{20}$$

Note that if $\mathbf{W}_w$ takes into account the environmental stiffness, minimization of the numerator amounts to assuming that the mechanism apply, for the given joint torques, the wrench that minimizes the energy of elastic deformation. By using suitable projector matrices, one readily gets

$$\min_{\mathbf{x}_s} \mathbf{w}^T\mathbf{W}_w\mathbf{w} = \mathbf{x}_a^T\boldsymbol{\Gamma}_w^T\mathbf{P}_{(\boldsymbol{\Gamma}_s, W_w)}^T\mathbf{W}_w\mathbf{P}_{(\boldsymbol{\Gamma}_s, W_w)}\boldsymbol{\Gamma}_w\mathbf{x}_a.$$

Therefore, the worst-case active force manipulability analysis is reduced to studying the ratio

$$R_{af}^w = \frac{\begin{bmatrix} \mathbf{x}_a \\ \mathbf{x}_h \end{bmatrix}^T \left[\begin{array}{c|c} \boldsymbol{\Gamma}_w^T\mathbf{P}_{(\boldsymbol{\Gamma}_s, W_w)}^T\mathbf{W}_w\mathbf{P}_{(\boldsymbol{\Gamma}_s, W_w)}\boldsymbol{\Gamma}_w & \mathbf{0} \\ \hline \mathbf{0} & \mathbf{0} \end{array}\right] \begin{bmatrix} \mathbf{x}_a \\ \mathbf{x}_h \end{bmatrix}}{\begin{bmatrix} \mathbf{x}_a \\ \mathbf{x}_h \end{bmatrix}^T \left[\begin{array}{c|c} \boldsymbol{\Gamma}_\tau^T\mathbf{W}_\tau\boldsymbol{\Gamma}_\tau & \mathbf{0} \\ \hline \mathbf{0} & \boldsymbol{\Gamma}_h^T\mathbf{W}_\tau\boldsymbol{\Gamma}_h \end{array}\right] \begin{bmatrix} \mathbf{x}_a \\ \mathbf{x}_h \end{bmatrix}}$$

that is again a generalized eigenvalue problem. The discussion of the ellipsoid is similar to the one given above for kinematic manipulability. Note that the numerator quadratic form has a number of zero eigenvalues equal to the components of $\mathbf{x}_h$, corresponding to joint torques balanced by purely internal contact forces, with no net effect on the object balance, that obviously give zero efficiency. If applied to the mechanism in Fig. 3, this analysis would assign maximum efficiency to forces pushing horizontally, and zero efficiency in the vertical direction: this result is consistent with the intuitive notion of active force manipulability illustrated in Fig. 3(a).

B. Passive Force Manipulability

For a given equilibrium wrench acting externally on the reference member, i.e., for given $\mathbf{x}_a$ and $\mathbf{x}_s$ in (19), the corresponding joint torques are not uniquely defined if a nullspace of $\mathbf{G}$ (internal contact forces) exists. However, it is reasonable to assume that the controller policy will specify that the torque with minimum cost be chosen to oppose a given wrench. The optimized passive force efficiency will hence be given by

$$R_{pf}^o = \frac{\mathbf{w}^T\mathbf{W}_w\mathbf{w}}{\min_{x_h} \boldsymbol{\tau}_a^T\mathbf{W}_\tau\boldsymbol{\tau}_a}. \tag{21}$$

Using the projector notation above established, one gets

$$\min_{x_h} \boldsymbol{\tau}_a^T\mathbf{W}_\tau\boldsymbol{\tau}_a = \mathbf{x}_a^T\boldsymbol{\Gamma}_\tau^T\mathbf{P}_{(\boldsymbol{\Gamma}_h, W_\tau)}^T\mathbf{W}_\tau\mathbf{P}_{(\boldsymbol{\Gamma}_h, W_\tau)}\boldsymbol{\Gamma}_\tau\mathbf{x}_a$$

and the optimized passive force manipulability analysis is studied by the ratio shown below

$$R^o_{pf} = \frac{\begin{bmatrix}\mathbf{x}_a\\ \mathbf{x}_s\end{bmatrix}^T \left[\begin{array}{c|c}\mathbf{\Gamma}_w^T\mathbf{W}_w\mathbf{\Gamma}_w & \mathbf{0}\\ \hline \mathbf{0} & \mathbf{\Gamma}_s^T\mathbf{W}_w\mathbf{\Gamma}_s\end{array}\right] \begin{bmatrix}\mathbf{x}_a\\ \mathbf{x}_s\end{bmatrix}}{\begin{bmatrix}\mathbf{x}_a\\ \mathbf{x}_s\end{bmatrix}^T \left[\begin{array}{c|c}\mathbf{\Gamma}_\tau^T\mathbf{P}^T_{(\mathbf{\Gamma}_h, W_\tau)}\mathbf{W}_\tau\mathbf{P}_{(\mathbf{\Gamma}_h, W_\tau)}\mathbf{\Gamma}_\tau & \mathbf{0}\\ \hline \mathbf{0} & \mathbf{0}\end{array}\right] \begin{bmatrix}\mathbf{x}_a\\ \mathbf{x}_s\end{bmatrix}}$$

where again $\Gamma_w^T\mathbf{W_w}\Gamma_s = 0$ is used. Note that the denominator quadratic form has a number of zero eigenvalues equal to the components of $\mathbf{x}_s$, corresponding to wrenches balanced by structural constraints, with no net effect on the active joints [nor on the passive, because of the equilibrium condition (15), that obviously give infinite efficiency. If applied to the mechanism in Fig. 3, this analysis would assign maximum (actually infinite) efficiency to forces pushing vertically, and smaller efficiency in the horizontal direction, consistently with the intuitive notion of passive force manipulability illustrated in Fig. 3(b).

C. Internal Force Manipulability

According to (19), the subspace of internal forces coincides with $\ker(\mathbf{G})$ and corresponds to the column space of matrix $\mathbf{\Gamma}_{fh}$, while the associated actuated joint torque subspace corresponds to the column space of $\mathbf{\Gamma}_h$. Notice that $\mathbf{\Gamma}_{fh}$ does not depend (for statically determinate mechanisms) on the system Jacobian, nor as a consequence, on the finger joint positions $\mathbf{q}$. An explicit one-to-one mapping between internal forces $\mathbf{f}_h \stackrel{\text{def}}{=} \mathbf{\Gamma}_{fh}\mathbf{x}_h$ and joint torques $\boldsymbol{\tau}_{ah} \stackrel{\text{def}}{=} \mathbf{\Gamma}_h\mathbf{x}_h$ exists such that the internal force manipulability index can be defined as the ratio of a performance measure in the space of $\mathbf{f}_h$'s, and an effort measure in the space of $\boldsymbol{\tau}_{ah}$'s

$$R_{fh} = \frac{\mathbf{f}_h^T\mathbf{W}_{th}\mathbf{f}_h}{\boldsymbol{\tau}_{ah}^T\mathbf{W}_{\tau h}\boldsymbol{\tau}_{ah}}. \tag{22}$$

The study of internal forces manipulability ellipsoids reduces to studying the ratio

$$R_{fh} = \frac{\mathbf{x}_h^T\mathbf{\Gamma}_{fh}^T\mathbf{W}_{th}\mathbf{\Gamma}_{fh}\mathbf{x}_h}{\mathbf{x}_h^T\mathbf{\Gamma}_h^T\mathbf{W}_{\tau h}\mathbf{\Gamma}_h\mathbf{x}_h} \tag{23}$$

which can be straightforwardly addressed along the lines of previous cases.

It is important to point out that, for mechanisms including unilateral and/or frictional contact constraints (such as is the case in dextrous manipulation) internal forces may have a fundamental role in avoiding that contacts are broken or slip. Typically, in order to fulfill such constraints, components of the internal force vector $\mathbf{f}_h$ must belong to some nonlinearly-bounded subset of the image of $\mathbf{\Gamma}_h$. In [2], such subset was shown to be convex, and an efficient algorithm to find the internal force vector $\hat{\mathbf{f}}_h$ maximizing a distance from the subset boundaries was provided. The "optimal" vector $\hat{\mathbf{f}}_h$ depends in general on matrix $\mathbf{G}$ and on the applied wrench $\mathbf{w}$, but not on the system Jacobian $\mathbf{J}$. Because $\mathbf{\Gamma}_{fh}$ is full rank and $\hat{\mathbf{f}}_h \in \mathtt{range}(\mathbf{\Gamma}_{fh})$, there exists a unique $\hat{\mathbf{x}}_h$ such that $\hat{\mathbf{f}}_h = \mathbf{\Gamma}_{fh}\hat{\mathbf{x}}_h$. The ratio $R_{fh}(\mathbf{x}_h)$ should therefore be evaluated at $\mathbf{x}_h = \hat{\mathbf{x}}_h$. The utility of (23) is hence to find the "best" configuration $\mathbf{q}$ of the hand for a given grasp, which minimizes the actuator effort necessary to exert the optimal contact force $\hat{\mathbf{f}}_h$, through modification of $\mathbf{\Gamma}_h(\mathbf{q})$. This amounts to maximizing $R_{fh}(\hat{\mathbf{x}}_h)$ as a function of $\mathbf{q}$, i.e., aligning the major axis of the ellipsoid in (23) with $\hat{\mathbf{x}}_h$.

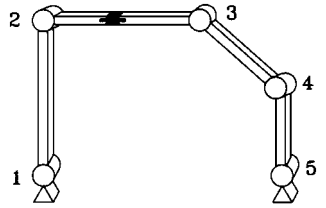

Fig. 4. A five-bar linkage used as a case study.

D. Duality

In the treatment of kinematic and force manipulability conducted so far, the usual duality relationship between kinematic and force ellipsoids is somewhat concealed. Indeed, for mechanisms such as those considered in this paper, the kinematic and force domains do have differences in practice. While the existence of $\ker(\mathbf{G})$ (internal forces) and $\ker(\mathbf{J}^T)$ (zero-torque contact forces) is the norm in practical devices, existence of a redundancy subspace $\ker(\mathbf{J})$ is not so frequent, and systems with nontrivial $\ker(\mathbf{G}^T)$, (contact) indeterminacy, are exceptional. This explains why the two domains have been treated differently.

Kineto-static duality for R^{ow}_k (13) is revealed when considering, in the force domain, the *worst-case* (w.r.t. structural forces), *optimized* (w.r.t. internal forces) efficiency index

$$R^{ow}_f = \frac{\min_{x_s}\ \mathbf{w}^T\mathbf{W}_w\mathbf{w}}{\min_{x_h}\ \boldsymbol{\tau}_a^T\mathbf{W}_\tau\boldsymbol{\tau}_a} = \frac{\mathbf{x}_a^T\mathbf{\Gamma}_w^T\mathbf{P}^T_{(\mathbf{\Gamma}_s, W_w)}\mathbf{W}_w\mathbf{P}_{(\mathbf{\Gamma}_s, W_w)}\mathbf{\Gamma}_w\mathbf{x}_a}{\mathbf{x}_a^T\mathbf{\Gamma}_\tau^T\mathbf{P}^T_{(\mathbf{\Gamma}_h, W_\tau)}\mathbf{W}_\tau\mathbf{P}_{(\mathbf{\Gamma}_h, W_\tau)}\mathbf{\Gamma}_\tau\mathbf{x}_a}. \tag{24}$$

Indeed, when (13) and (24) are compared assuming $\mathbf{W}_u\mathbf{W}_w = \mathbf{W}_q\mathbf{W}_\tau$, it is found that the Rayleigh ratios (13) and (24) have numerator and denominator exchanged (this can be verified considering that, because of the principle of virtual work, it holds $\mathbf{\Gamma}_{oc}^T\mathbf{\Gamma}_w = \mathbf{\Gamma}_{qc}^T\mathbf{\Gamma}_\tau$, $\mathbf{\Gamma}_\tau^T\mathbf{\Gamma}_r = \mathbf{\Gamma}_{qc}^T\mathbf{\Gamma}_h = \mathbf{\Gamma}_i^T\mathbf{\Gamma}_w = \mathbf{\Gamma}_s^T\mathbf{\Gamma}_{oc} = 0$).

V. Case Studies

A. Five-Bar Linkage

As a first case study, consider a five-bar closed chain described as a two-arm cooperating system (see Fig. 4). We want to investigate the effects on kinematic and force manipulability of different design choices about the number and the location of actuators at the joints of the chain. In particular, we will compare two designs with two actuators placed at joints 1 and 5 (see Fig. 5), and at joints 2 and 4 (see Fig. 6), respectively, and a fully actuated design (see Fig. 7). Comparisons will be made about the nominal configuration depicted in Fig. 4, for which contact points coordinates are $c_{p1} = [-(2/3), 0]$ and $c_{p2} = [-(1/3), 0]$, contact types are modeled as complete constraints, the object frame origin is at $[-(1/2), 0]$, and the coordinates of the centers of the five joints are $\mathbf{o}_1 = [-1 \quad -2]$,

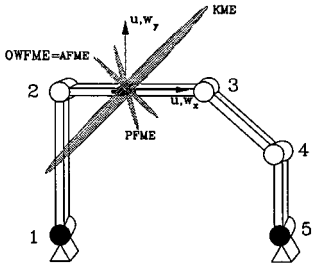

Fig. 5. The five-bar linkage with joints 1 and 5 actuated, along with kinematic, active force, and passive force manipulability ellipsoids.

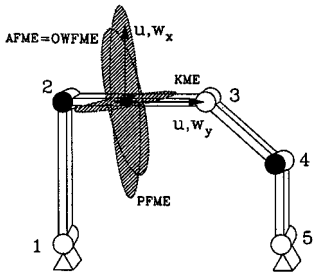

Fig. 6. The five-bar linkage with joints 2 and 4 actuated and the kinematic and force manipulability ellipsoids.

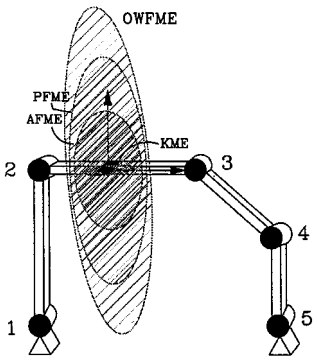

Fig. 7. The five-bar linkage with all the joints actuated and the kinematic and force, and manipulability ellipsoids.

$\mathbf{o}_2 = [-1 \quad 0]$, $\mathbf{o}_3 = [0 \quad 0]$, $\mathbf{o}_4 = [1 \quad -1]$, $\mathbf{o}_5 = [1 \quad -2]$. For simplicity's sake, we will consider all weight matrices as identities.

By easy computations, it is checked that $\ker(\mathbf{G}^T) = \ker(\mathbf{J}) = \mathbf{0}$, hence the system in Fig. 4 has no indeterminacy ($\mathbf{\Gamma}_i = \mathbf{0}$) nor redundancy ($\mathbf{\Gamma}_{a,r} = \mathbf{\Gamma}_{ap,c} = \mathbf{\Gamma}_{pa,c} = \mathbf{0}$), while the dimension of the subspace of internal forces $\ker(\mathbf{G})$ is 3, and the dimension of the subspace of zero-torque wrenches $\ker(\mathbf{J}^T)$ is 1.

1) Actuators at Joints 1 and 5: If only joints 1 and 5 are actuated (see Fig. 5), the two generalized eigenvalues of the kinematic manipulability ellipsoid (11) evaluate to 9.74 and 0.51. The projection of the kinematic ellipsoid (KME) onto the plane $(\mathbf{u}_x, \mathbf{u}_y)$ is reported in Fig. 5. In the force domain, the active force ellipsoid (20) has two eigenvalues which evaluate to 1.95 and 0.10. The projection of the active force manipulability ellipsoid onto the $(\mathbf{w}_x, \mathbf{w}_y)$-plane (AFME) is reported in Fig. 5. The eigenvalues of the passive force ellipsoid are computed as 2.04, 0.11, and ∞. The latter eigenvalue corresponds to an external wrench (in direction $[0, -0.89, 0.45]^T$) resisted by the mechanism with zero torques: the passive force ellipsoid (21) degenerates to a cylinder whose intersection with the plane $(\mathbf{w}_x, \mathbf{w}_y)$ is the PFM ellipse represented in Fig. 5.

The subspace of reachable internal forces is trivial in this case ($\mathbf{\Gamma}_{fh} = \mathbf{\Gamma}_h = \mathbf{0}$), and duality is found between the kinematic manipulability ellipsoid and the active force ellipsoid.

2) Actuators at Joints 2 and 4: In this case, depicted in Fig. 6, the two generalized eigenvalues of the kinematic manipulability ellipsoid evaluate to 1.42 and 0.22. The projection of the kinematic ellipsoid (KME) onto the plane $(\mathbf{u}_x, \mathbf{u}_y)$ is reported in Fig. 6. In the force domain, the active force ellipsoid's eigenvalues are 4.55 and 0.70. The projection of the active force manipulability ellipsoid (AFME) is reported in Fig. 6. The passive force ellipsoid degenerates to a cylinder whose intersection with the $(\mathbf{w}_x, \mathbf{w}_y)$-plane is reported in Fig. 6. The efficiency indexes are $[0.76, 4.90, \infty]$. No internal forces ($\mathbf{\Gamma}_{fh} = \mathbf{\Gamma}_h = \mathbf{0}$) are present in the mechanism and, as for the previous case, the kinematic manipulability is dual to the active force ellipsoid.

3) Actuators at All Joints: If all joints are actuated (Fig. 7), the kinematic manipulability ellipsoid is described by two generalized eigenvalues, 0.59 and 0.11. The projection of the kinematic ellipsoid (KME) onto the plane (u_x, u_y) is reported in Fig. 7. The active force ellipsoid has eigenvalues 1.38 and 4.68. The projection of the active force manipulability ellipsoid (AFME) is reported in Fig. 7. The passive force ellipsoid degenerates to a cylinder whose intersection with the $(\mathbf{w}_x, \mathbf{w}_y)$-plane is reported in Fig. 7. The efficiency indexes are $[1.75, 8.95, \infty]$. Differently from previous cases, here, the mechanism exhibits a three-dimensional subspace of reachable internal forces ($\mathbf{\Gamma}_h \neq \mathbf{0}$) along with the one-dimensional subspace of structural forces ($\mathbf{\Gamma}_s \neq \mathbf{0}$). Duality is found between the kinematic manipulability ellipsoid and the optimized worst-force ellipsoid (24) whose generalized eigenvalues are 1.7 and 8.79. The projection (denoted with OWFME) on the $(\mathbf{w}_x, \mathbf{w}_y)$-plane of this ellipsoid is reported in Fig. 7. Finally, regarding internal forces, the manipulability ellipsoid described in (23) is three-dimensional and its eigenvalues are $[0.14 \quad 1.2 \quad 0.63]$.

4) Analysis of Results: Based on the results of manipulability analysis, some distinctive features of the three different designs are put into evidence. Actuators placed at joints 1 and 5 provide an elongated KME, with very high efficiency (9.74) in one direction, and much lower elsewhere. Actuators placed at joints 2 and 4 provide lower highest efficiency (1.42), and higher lowest efficiency (0.22), i.e., a more balanced design. The geometric information contained in the eigenvectors is also useful: for instance, if the task of the mechanism was to swipe fast in the horizontal direction, while keeping precise positioning in the vertical direction, then the second design would clearly be superior, because of a combination of Yoshikawa's and Salisbury–Craig's interpretations.

The design with all joints actuated provides lower eigenvalues than both other designs. An intuitive explanation for this fact is that, for any given velocity of the object, all five actuators have to be controlled to nonzero velocity to comply with the motion, and their velocity represent a cost in the Yoshikawa's efficiency

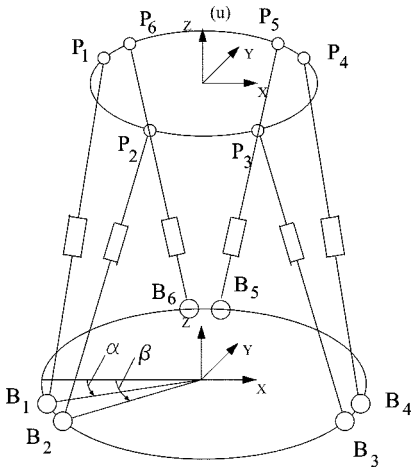

Fig. 8. The model of a 6-DOF Stewart platform.

index. On the other hand, an advantage of having redundant actuation is apparent in the possibility of achieving a more balanced design (rounder ellipsoid), and overall a much better accuracy in the Salisbury–Craig's spirit.

In the force domain, analogous considerations apply. It is to be noticed that in none of the above cases active and passive force ellipsoids coincide, the difference being larger in the 1–5 design.

B. Stewart Platform

In this section, tools for manipulability analysis developed so far are applied to optimize the design of a Stewart platform (see Fig. 8). The goal of optimized design is to find a placement of the legs endpoints, such that the kinematic manipulability ellipsoid evaluated at a reference configuration of the platform, is as similar as possible to a prescribed ellipsoid, which is chosen (as suggested in [18]) so as to incorporate the task specifications.

Let the reference configuration of the platform have origin at $\mathbf{p}_0 = (0,\, 0,\, 2)m$ and $\mathbf{R}_0 = \mathbf{I}$. Also, we assume for simplicity $\mathbf{W}_q$ to be the identity matrix (in the chosen reference and measurement units), and let the desired task ellipsoid in the space of end-effector twists $\dot{\mathbf{u}}$ be isotropic in the translation components and in the orientation components, namely

$$\mathbf{W}_{\text{task}} = \text{diag}\left(1\frac{\text{m}^2}{\text{s}^2}, 1\frac{\text{m}^2}{\text{s}^2}, \frac{\text{m}^2}{\text{s}^2}, 0.2\frac{\text{rad}^2}{\text{s}^2}, 0.2\frac{\text{rad}^2}{\text{s}^2}, 0.2\frac{\text{rad}^2}{\text{s}^2}\right).$$

The problem is to find the design which makes the platform's kinematic ellipsoid

$$\frac{\dot{\mathbf{u}}^T \mathbf{W}_u \dot{\mathbf{u}}}{\dot{\mathbf{q}}^T \mathbf{W}_q \dot{\mathbf{q}}}$$

with $\mathbf{W}_u = \mathbf{W}_{\text{task}}^{-1}$, as close to a unit sphere as possible.

In order to have a scalar cost to minimize with respect to the design parameters, we choose (with some degree of arbitrariness which is unfortunately unavoidable) the sum of square errors between the maximum and minimum eigenvalues of the ellipsoids

$$C = (\lambda_{\max} - 1)^2 + (\lambda_{\min} - 1)^2 .$$

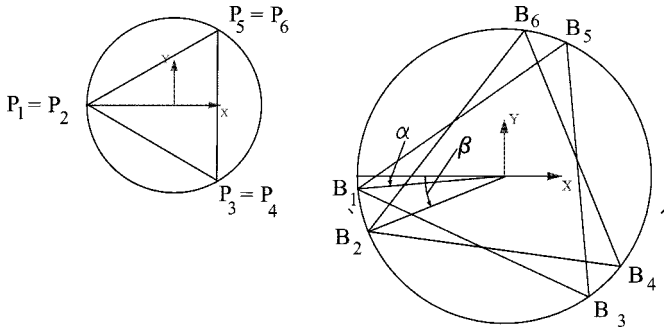

Fig. 9. Angles α and β used as parameters in the design of a Stewart platform.

According to our cooperating manipulation paradigm, the platform is regarded here as a system of six limbs (legs), each with three unactuated joints (forming a spherical joint at the base of the leg) and one actuated prismatic joint in their middle. Let B_i denote the position of the ith spherical joint at the base, and P_i the position of the ith contact joint on the upper platform. Joints at P_i are modeled as soft-finger contacts with contact normal $\mathbf{z}_i$ directed along the corresponding leg's axis joining P_i and B_i. Notice that, should spherical joints be used for upper joints, a six-dimensional subspace of kinematically indeterminate motions of the system would result, consisting of rotations of the legs about their axes, which are unwanted.

The optimization problem variables are the positions P_i and B_i, $i = 1, \cdots, 6$. To reduce the dimensionality of the problem, however, we fix positions of the upper joints P_i, with consecutive pairs coincident at the vertices of an equilateral triangle inscribed into a circle of radius 1.5 m. The lower joints with odd index, and those with even index, are placed at the vertices of two equilateral triangles inscribed into a circle of radius 2 m (see Fig. 9). The triangle of vertices $(\mathbf{B}_1, \mathbf{B}_3, \mathbf{B}_5)$ is placed at an angle α w.r.t. to the x-axis of the base frame, while the triangle of vertices $(\mathbf{B}_2, \mathbf{B}_4, \mathbf{B}_6)$ is placed at an angle β.

In a generic design (α, β), the platform exhibits no indeterminacy ($\mathbf{\Gamma}_{ii}$ is zero), see (10). However, a kinematic indeterminacy ($\mathbf{\Gamma}_{ii} \neq \mathbf{0}$) appears for *singular* parameter sets [9]. In the case of Fig. 9, singularity appears when $\beta = \alpha$. Singularity generates kinematic indeterminacy, i.e., a nonvoid block $\mathbf{\Gamma}_{op,\,i}$, making platform and passive joints motions even with active joints locked. Obviously, as pointed out in [16], indeterminacy should be avoided in practical device design. At singularities $\beta = \alpha$, the kinematic ellipsoid in (11) exhibits three infinite generalized eigenvalues whose eigenvectors are the indeterminate (or singular) directions of the mechanism. From a geometric point of view, when $\alpha = \beta = 0$ all legs intersect at a single point, which represents a particular case in Hunt's description of singularities for parallel robots ([7]).

The inverse of cost C is plotted in Fig. 10. Numerical estimates of optimal design parameters are obtained as ($\alpha_1 = 1°$, $\beta_1 = -120°$), corresponding to point M_1 in Fig. 10, and ($\alpha_2 = 1°$, $\beta_2 = 120°$) (M_2). At these points, the same scalar cost is attained ($C = 1/1.67$), as they represent symmetric configurations.

The resulting active kinematic manipulability ellipsoid evaluated at the optimum ($\alpha_2 = 1°$, $\beta_2 = 120°$) has the following

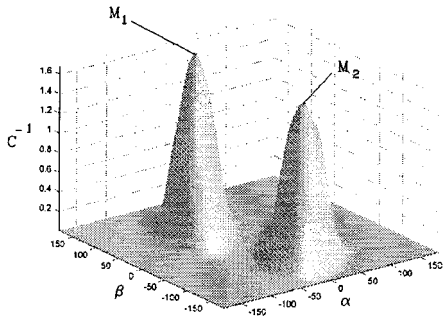

Fig. 10. Optimization results for a 2-DOF design of a Stewart platform. Best designs with respect to the chosen criterion correspond to higher values of the inverse cost function.

eigenvalues

$$[1 \quad 1 \quad 0.98 \quad 0.23 \quad 0.23 \quad 0.23]$$

with corresponding eigenvectors (in the space of platform twists)

$$\begin{bmatrix} -8 & -92 & 8 & 1 & 10 & -2 \\ 6 & -126 & -5 & 3 & 1 & 1 \\ -2 & -1 & -8 & 3 & -78 & -4 \\ 1 & 29 & -1 & 11 & 45 & -6 \\ -2 & 15 & 1 & 10 & -17 & 8 \\ -4 & -3 & -19 & -1 & 35 & 2 \end{bmatrix}.$$

Note that the resulting ellipsoid is not very close to the desired shape and size, it is however the best possible approximation (in the sense specified by the cost C) given the constraints imposed on the design.

In the force domain, for generic α and β, there are no wrenches that can be balanced with zero actuator torques ($\mathbf{\Gamma}_s$ and $\mathbf{\Gamma}_{fs}$ are void). It is noteworthy that, although the nullspace of the grasp matrix $\mathbf{G}$ is 12-dimensional, the subspace of active internal forces is trivial ($\mathbf{\Gamma}_h$ and $\mathbf{\Gamma}_{fh}$ are void). As a consequence of these facts, there is no difference between passive and active force manipulability, and both are dual to the kinematic case.

VI. Conclusions

In this paper, we have extended some tools developed in the robotic literature for the analysis of manipulability of serial-chain manipulators to more general mechanisms, including closed chains with free kinematic pairs. Results allow to attack the manipulability analysis of many more mechanisms than previously possible, and are applied to the study of optimized design of a five-bar closed-chain mechanism, and of a Stewart platform. Further study is necessary to address some important open problems, such as second order manipulability analysis, and manipulability of systems with nonholonomic constraints, such as, e.g., cooperating wheeled vehicles.

Appendix A
Notation

Let $s = 2$, $d = 3$ for 2-D mechanisms, and $s = 3$, $d = 6$ for 3-D ones. Let q_a, q_p be the number of actuated and passive joints, respectively, and $q \stackrel{\text{def}}{=} q_a + q_p$. Let n the number of contacts, and set

$$\dot{\mathbf{q}} = [\dot{q}_1, \dot{q}_2, \cdots, \dot{q}_q]^T, \qquad \dot{\mathbf{q}} \in \mathbb{R}^q$$
$$\boldsymbol{\tau} = [\boldsymbol{\tau}_1, \boldsymbol{\tau}_2, \cdots, \boldsymbol{\tau}_q]^T, \qquad \boldsymbol{\tau} \in \mathbb{R}^q$$
$$\dot{\mathbf{u}} = \left[\mathbf{v}^T, \omega^T\right]^T, \qquad \dot{\mathbf{u}} \in \mathbb{R}^d$$
$$\mathbf{w} = \left[\mathbf{f}^T, \mathbf{m}^T\right]^T, \qquad \mathbf{w} \in \mathbb{R}^d$$

where $\mathbf{v}$ (ω) is the linear (angular) velocity of the object and $\mathbf{f}$ ($\mathbf{m}$) is the force (moment) on the object.

Let matrix $\tilde{\mathbf{J}}$ represent the aggregated Jacobian of the mechanism limbs, i.e., the linear map between joint velocities and the velocities (in all directions) of frames attached to limbs at contact points; and analogously, let $\tilde{\mathbf{G}}^T$ be the object grasp matrix, mapping object velocities into velocities of contact frames on the object (for a constructive description of these matrices, see, e.g., [1]). Rigid-body contact constraints of different types can be written as

$$\mathbf{H}\left(\tilde{\mathbf{J}}\dot{\mathbf{q}} - \tilde{\mathbf{G}}^T\dot{\mathbf{u}}\right) = \mathbf{J}\dot{\mathbf{q}} - \mathbf{G}^T\dot{\mathbf{u}} = 0$$

TABLE I
Selectors for Different Contact Types

Contact Type	Force Selector FS_i	Moment Selector MS_i
Point Contact w/o Friction	$\mathbf{z}_i^T$	$\mathbf{0}_{1\times(d-s)}$
Point Contact w/h Friction (Hard–Finger)	$\mathbf{I}_s$	$\mathbf{0}_{1\times(d-s)}$
Line Contact w/o Friction	$\mathbf{z}_i^T$	$(S(\mathbf{z}_i)\mathbf{x}_i)^T$
3D Line Contact w/h Friction	$\mathbf{z}_i^T$	$\begin{bmatrix} (S(\mathbf{z}_i)\mathbf{x}_i)^T \\ \mathbf{z}_i^T \end{bmatrix}$
3D Planar Contact w/o Friction	$\mathbf{z}_i^T$	$\begin{bmatrix} \mathbf{x}_i^T \\ \mathbf{y}_i^T \end{bmatrix}$
Planar Contact w/h Friction (Complete–Constraint)	$\mathbf{I}_s$	$\mathbf{I}_{d-s}$
3D Soft Finger	$\mathbf{I}_3$	$\mathbf{z}_i^T$

TABLE II
Selectors for Different Joint Types

Joint Type	Force Selector FS_i	Moment Selector MS_i
3D Rotoidal	$\mathbf{I}_3$	$\begin{bmatrix} \mathbf{x}_i^T \\ \mathbf{y}_i^T \end{bmatrix}$
2D Rotoidal	$\mathbf{I}_2$	0
3D Prismatic	$\begin{bmatrix} \mathbf{x}_i^T \\ \mathbf{y}_i^T \end{bmatrix}$	$\mathbf{I}_3$
2D Prismatic	$\mathbf{x}_i^T$	1
3D Spherical	$\mathbf{I}_3$	$\mathbf{0}_{1\times3}$

where the selection matrix $\mathbf{H}$ is built by removing all the zero rows from a matrix

$$\hat{\mathbf{H}} = \mathrm{diag}\left(\mathrm{FS}_1, \cdots, \mathrm{FS}_n, \mathrm{MS}_1, \cdots, \mathrm{MS}_n\right).$$

which is comprised of *force selector* (FS) and *moment selector* (MS) blocks, chosen according to different differential constraints between the limbs and the object. The range space of the transpose of a selector block represents directions in which relative velocities are prohibited by the constraint. Some examples of selector blocks are reported in Table I for some commonly encountered contact types, and in Table II for a few common kinematic joints. In Table I, vectors $\mathbf{z}_i$ represent the unit surface normal at the ith contact while $\mathbf{x}_i$ and $\mathbf{y}_i$ are two unit vectors defining the line and plane of contact. In Table II, vectors $\mathbf{x}_i$ and $\mathbf{y}_i$ denote two unit vectors normal to the joint axis $\mathbf{z}_i$.

REFERENCES

[1] A. Bicchi, C. Melchiorri, and D. Balluchi, "On the mobility and manipulability of general multiple limb robots," *IEEE Trans. Robot. Automat.*, vol. 11, pp. 215–228, Apr. 1995.

[2] A. Bicchi, "On the closure properties of robotic grasping," *Int. J. Robot. Res.*, vol. 14, no. 4, pp. 319–334, 1995.

[3] A. Bicchi, D. Prattichizzo, and C. Melchiorri, "Force and dynamic manipulability for cooperating robot systems," in *Proc. Int. Symp. on Robotic Systems (IROS'97)*, 1997, pp. 1479–1484.

[4] A. Bicchi and D. Prattichizzo, "Manipulability opf cooperating robots with passive joints," in *Proc. IEEE Int. Conf. on Robotics and Automatation*, 1998, pp. 1038–1044.

[5] P. Chiacchio, S. Chiaverini, L. Sciavicco, and B. Siciliano, "Global task space manipulability ellipsoids for multiple-arm systems," *IEEE Trans. Robot. Automat.*, vol. 7, pp. 678–685, Oct. 1991.

[6] G. H. Golub and C. F. VanLoan, *Matrix Computations*: Johns Hopkins University Press, 1989.

[7] K. H. Hunt, *Kinematic Geometry of Mechanisms*. Oxford, U.K.: Clarendon, 1978.

[8] S. Lee, "Dual redundant arm configuration optimization with task-oriented dual arm manipulability," *IEEE Trans. Robot. Automat.*, vol. 5, pp. 78–97, Feb. 1989.

[9] J. P. Merlet, "Singular configurations of parallel manipulators and Grassman geometry," *Int. J. Robot. Res.*, vol. 8, no. 5, pp. 45–56, 1989.

[10] C. Melchiorri, "Multiple whole-limb manipulation: An analysis in the force domain," *Int. J. Robot. Auton. Syst.*, vol. 20, no. 1, pp. 15–38, 1997.

[11] F. C. Park and J. W. Kim, "Manipulability and singularity analysis of multiple robot systems: A geometric approach," in *Proc. IEEE Int. Conf. on Robotics and Automation*, 1998, pp. 1032–1037.

[12] ——, "Kinematic manipulability of closed chains," in *Recent Advances in Robot Kinematics*, J. Lenarcic and V. Parenti-Castelli, Eds. Dordrecth, The Netherlands: Kluwer, 1996.

[13] J. K. Salisbury and J. J. Craig, "Articulated hands, force control and kinematic issues," *Int. J. Robot. Res.*, vol. 1, no. 1, pp. 4–17, 1982.

[14] G. Strang, *Linear Algebra and Its Applications*. Orlando, FL: Harcourt Brace Jovanovich, 1988.

[15] J. T. Wen and L. S. Wilfinger, "Kinematic manipulability of general constrained rigid multibody systems," *Proc. IEEE Int. Conf. on Robotics and Automation*, pp. 1020–1025, 1998.

[16] ——, "Kinematic manipulability of general constrained rigid multibody systems," *IEEE Trans. Robot. Automat.*, vol. 15, pp. 558–567, Apr. 1999.

[17] T. Yoshikawa, "Manipulability of robotics mechanisms," *Int. J. Robot. Res.*, vol. 4, no. 2, pp. 3–9, 1985.

[18] Z. Li, P. Hsu, and S. S. Sastry, "Grasping and coordinated manipulation by a multifingered robot hand," *Int. J. Robot. Res.*, vol. 8, no. 4, pp. 33–50, 1989.

Antonio Bicchi graduated from the University of Bologna, Bologna, Italy, in 1988.

From 1988 to 1990, he was a Postdoctoral Scholar at the M.I.T. Artificial Intelligence Laboratory. He is currently an Associate Professor of Systems Theory and Robotics in the Department of Electrical Systems and Automation (DSEA) of the University of Pisa, Pisa, Italy. Since 1990, he has been leading the Robotics Group at the Interdepartmental Research Center "E. Piaggio," University of Pisa. He has published more than 100 papers in international journals, books, and refereed conferences. His main research interests are in the field of dextrous manipulation, including force/torque and tactile sensing and sensory control, dynamics, kinematics and control of complex mechanichal systems, and motion planning and control for nonholonomic and quantized systems.

Domenico Prattichizzo (M'95) received the M.S. degree in electronics engineering and the Ph.D. degree in robotics and automation from University of Pisa, Pisa, Italy, in 1991 and 1995, respectively.

In 1994, he was a Visiting Scientist at the M.I.T. Artificial Intelligence Laboratory. He is currently an Assistant Professor at the Department of Information Engineering, University of Siena, Siena, Italy. Since 1991, he has been a Research Associate in the Robotics and Automation Group at the Interdepartmental Research Centro "E. Piaggio," University of Pisa, Pisa, Italy. He has published more than 60 papers in international journals, books, and refereed conferences. His research activities include grasping and dexterous manipulation, nonholonomic systems, optimal sensor design, active vision, and geometric control.

Dr. Prattichizzo was co-organizer and co-chairman of sessions on robotics in many international conferences.